Supporting Information

Tunable two-photon absorption near-infrared materials by different electron-donors and π-bridge center with applications in bioimaging in live cells

*Ming Kong,[a] Ting Wang,[b] Xiaohe Tian,[a] Fang Wang,[a] Yanqiu Liu,[a] Qiong Zhang,[a] Hui Wang,[a] Hongping Zhou,[a] Jieying Wu [*a] and Yupeng Tian [*a]*

[a] Department of Chemistry, Key Laboratory of Functional Inorganic Material Chemistry of Anhui Province, Anhui University, Hefei 230039, P. R. China

[b] School of Life Science, Anhui University, Anhui Province Key Laboratory of R&D of Chinese Medicine，Hefei, China

E-mail: jywu1957@163.com; yptian@ahu.edu.cn

S1. General methods

All chemicals were commercially available and used as obtained. The solvents were

purified by conventional methods before use. The ^{1}H NMR and ^{13}C NMR spectra recorded on at 25ºC using Bruker Avance 400 spectrometer were reported as parts per million (ppm) from TMS. IR spectra were recorded on NEXUS 870 (Nicolet) spectrophotometer in the 400-4000 cm^{-1} region using a powder sample on a KBr plate. Mass spectra were obtained on a Micromass MALDI-TOF-MS.

X-ray crystallography and structure solution. The X-ray diffraction measurements were performed on a Bruker SMART CCD area detector using graphite monochromated MoKα radiation (λ = 0.71069 Å) at 298(2) K. Intensity data were collected in the variable ω-scan mode. The structures were solved by direct methods and difference Fourier syntheses. The non-hydrogen atoms were refined anisotropically and hydrogen atoms were introduced geometrically. Calculations were performed with the SHELXTL-97 program package. Crystallographic data (excluding structure factors) for the structures reported in this paper have been deposited with the Cambridge Crystallographic Data Centre as supplementary publication no. CCDC number: **X1** (965153), **XT1** (991562), **XT2** (991563), **XT3** (991564). Details of the crystal parameters, data collections and refinements for the complexes are summarized in **Table 1** and selected bond distances and angles are listed in **supporting.**

Absorption and fluorescence spectra. Absorption spectra were obtained on a UV-265 spectrophotometer, Fluorescence measurements were performed using a Hitachi F-7000 fluorescence spectrophotometer excited at the longest absorption band with a 1 cm standard quartz cell. The concentration of sample solution was 1.0×10^{-5} mol/L. The excitation and emission slit widths were all 5 nm. For time-resolved fluorescence measurements, the fluorescence signals were collimated and focused onto the entrance slit of a monochromator with the output plane equipped with a photomultiplier tube (HORIBA HuoroMax-4P). The decays were analyzed by 'least-squares'. The quality of the exponential fits was evaluated by the goodness of fit (χ^2).

Theoretical calculation. To better identify the charge transition, time-dependent density functional theory (TD-DFT) calculations were carried out in ethanol. Geometry optimizations (**X2** and **X3**) were carried out with B3LYP functional

without any symmetry restraint, and the TD-DFT calculations were performed on the optimized structure with B3LYP functional. For **X1**, **XT1**, **XT2** and **XT3**, the crystal structures were directly adopted for TD-DFT calculations. All calculations, including optimizations and TD-DFT, were performed with the G03 software. Geometry optimization of the singlet ground state and the TD-DFT calculation of the lowest 50 singlet-singlet excitation energies were calculated with a basis set composed of 6-31 G for C H N O S atoms. An analytical frequency confirmed evidence that the calculated species represents a true minimum without imaginary frequencies on the respective potential energy surface. The lowest 40 spin-allowed singlet-singlet transitions, up to energy of about 5 eV, were taken into account in the calculation of the absorption spectra.

Fluorescence quantum yield

The fluorescence quantum yield was measured by using

$$\Phi_s = \Phi_r \left(\frac{A_r \eta_s^2 D_s}{A_s \eta_r^2 D_r} \right)$$

in which the subscripts *s* and *r* stand for designate the sample and reference sample, respectively, A is the absorbance at λ_{exc}, η is the average refractive index of the appropriate solution, and D is the integrated fluorescence area under the corrected emission spectrum. Here, quinine sulfate in 1 N H_2SO_4 was used as the reference (Φ=0.54). All the measurements were at room temperature.

Microscopy. HepG2 cells were imaged on a Zeiss LSM 710 META upright confocal laser scanning microscope using magnification 40× and 100× water-dipping lenses for monolayer cultures. Image data acquisition and processing was performed using Zeiss LSM Image Browser, Zeiss LSM Image Expert and Image J.

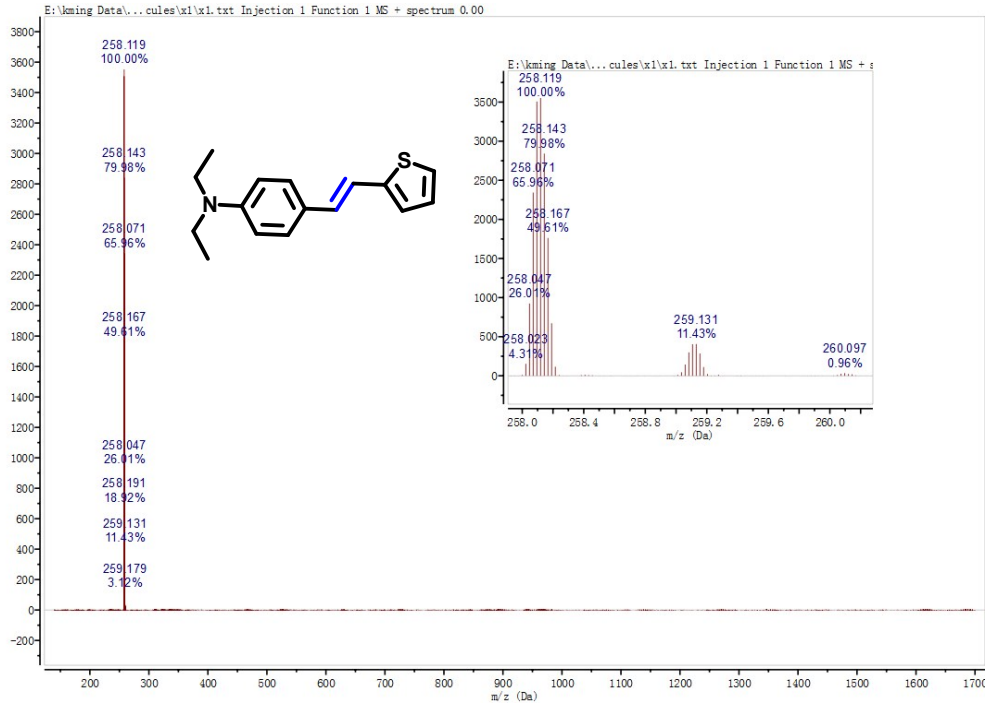

Figure S1. MALDI-TOF-MS of **X1**

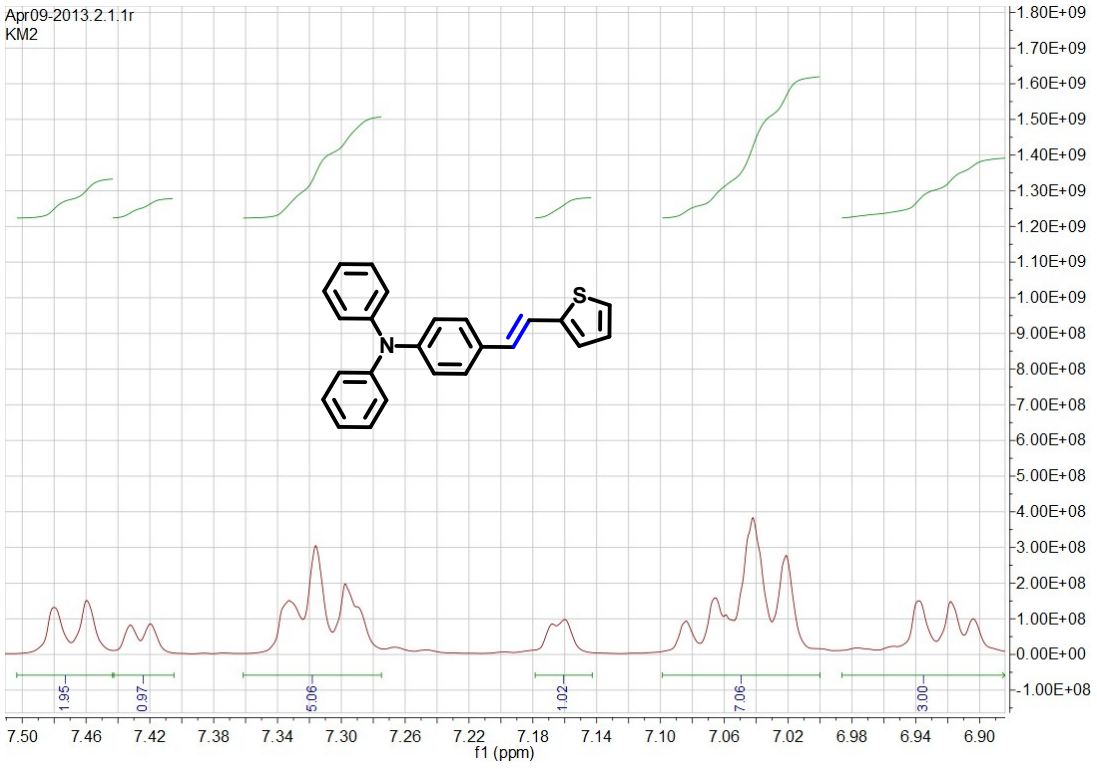

Figure S2. ^{1}H NMR of **X2**

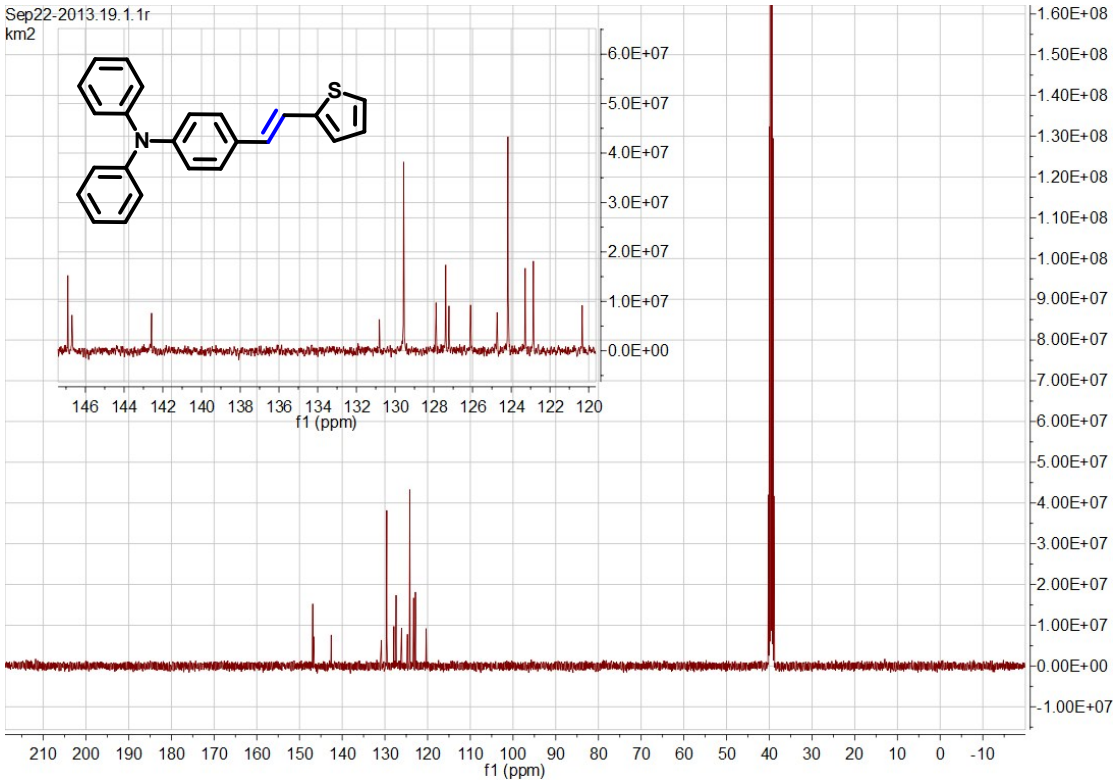

Figure S3. ^{13}C NMR of **X2**

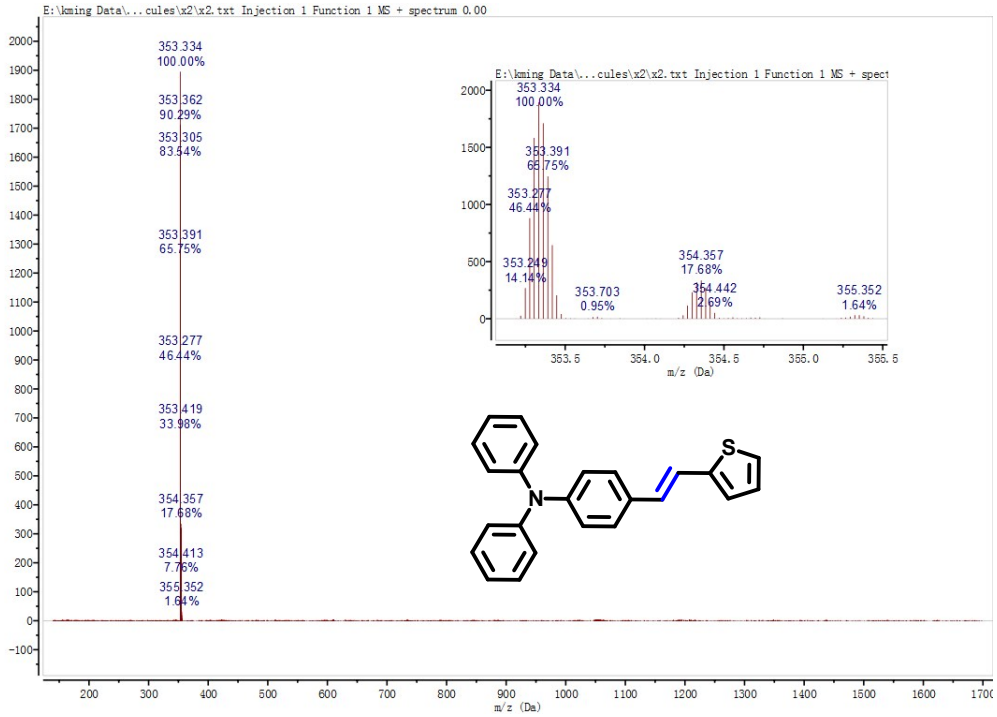

Figure S4. MALDI-TOF-MS of **X2**

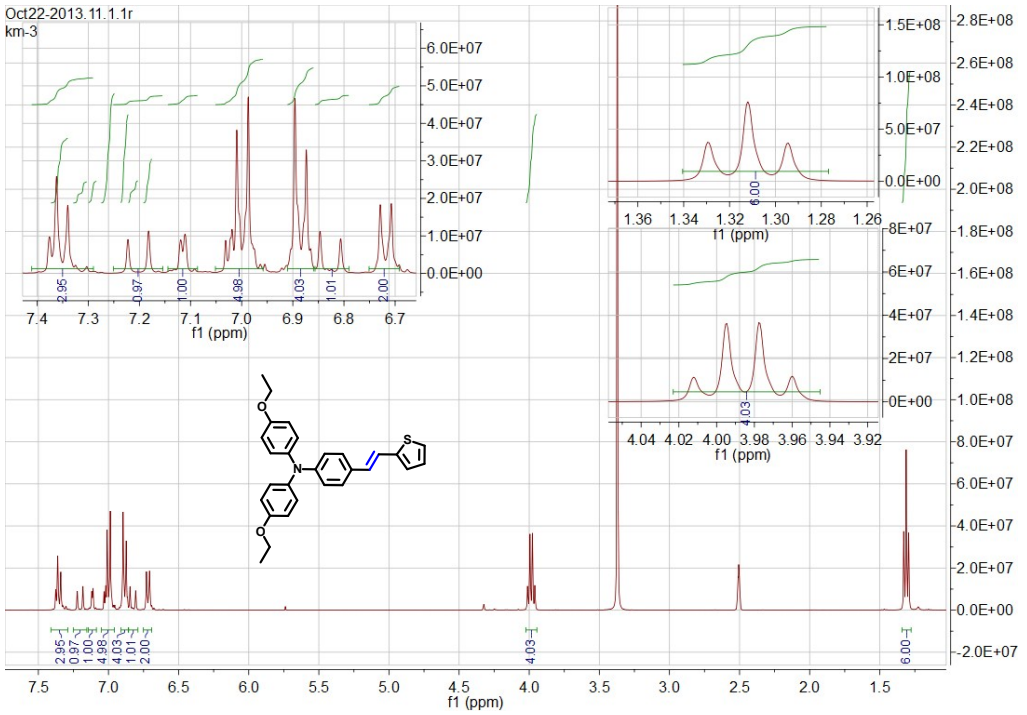

Figure S5. ^{1}H NMR of **X3**

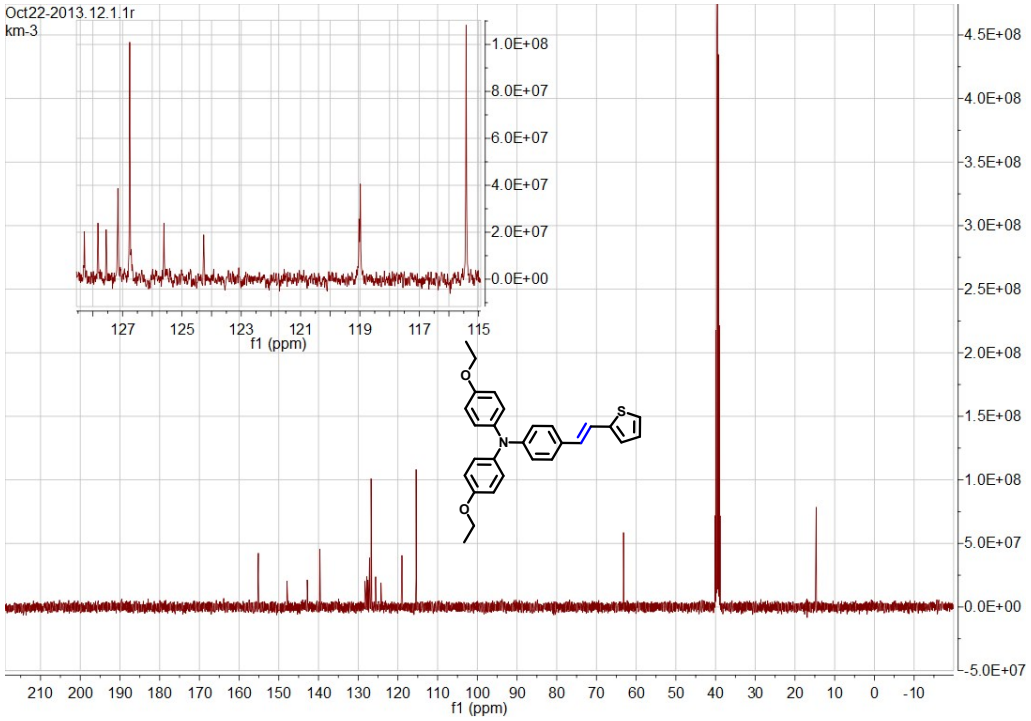

Figure S6. ^{13}C NMR of **X3**

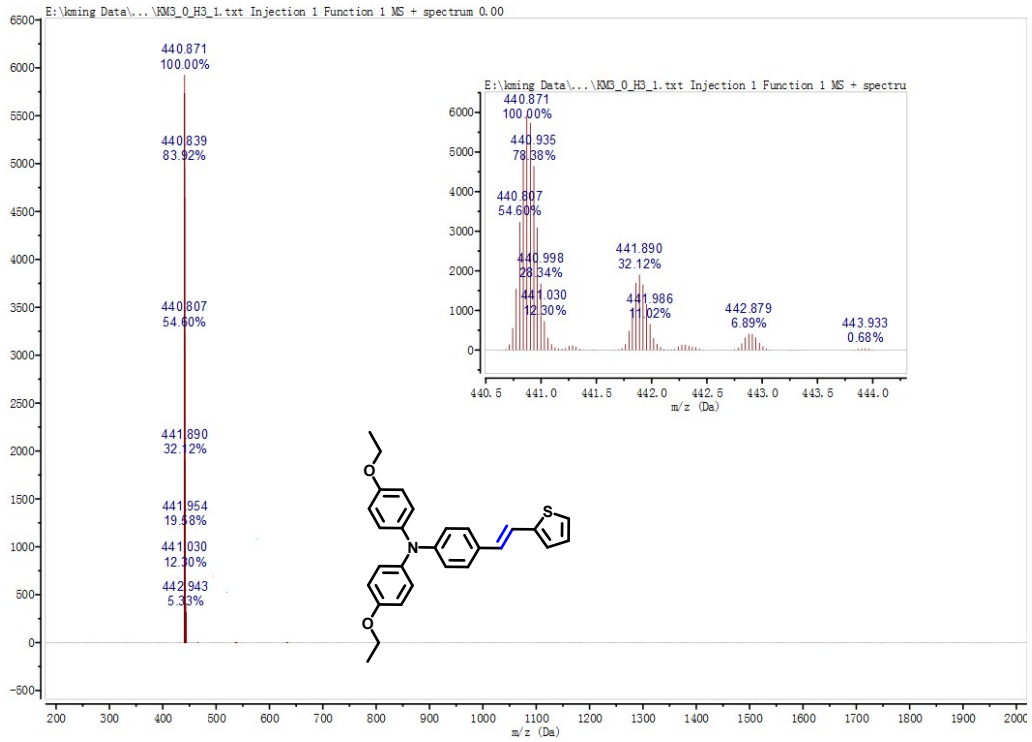

Figure S7. MALDI-TOF-MS of **X3**

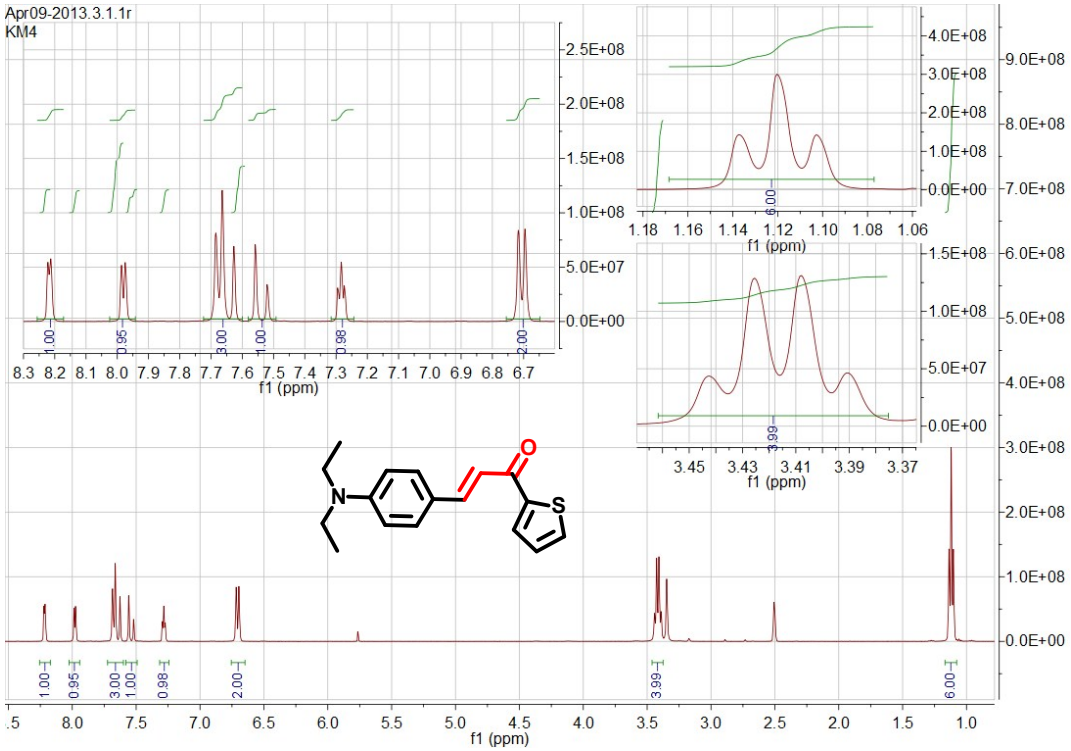

Figure S8. ^{1}H NMR of **XT1**

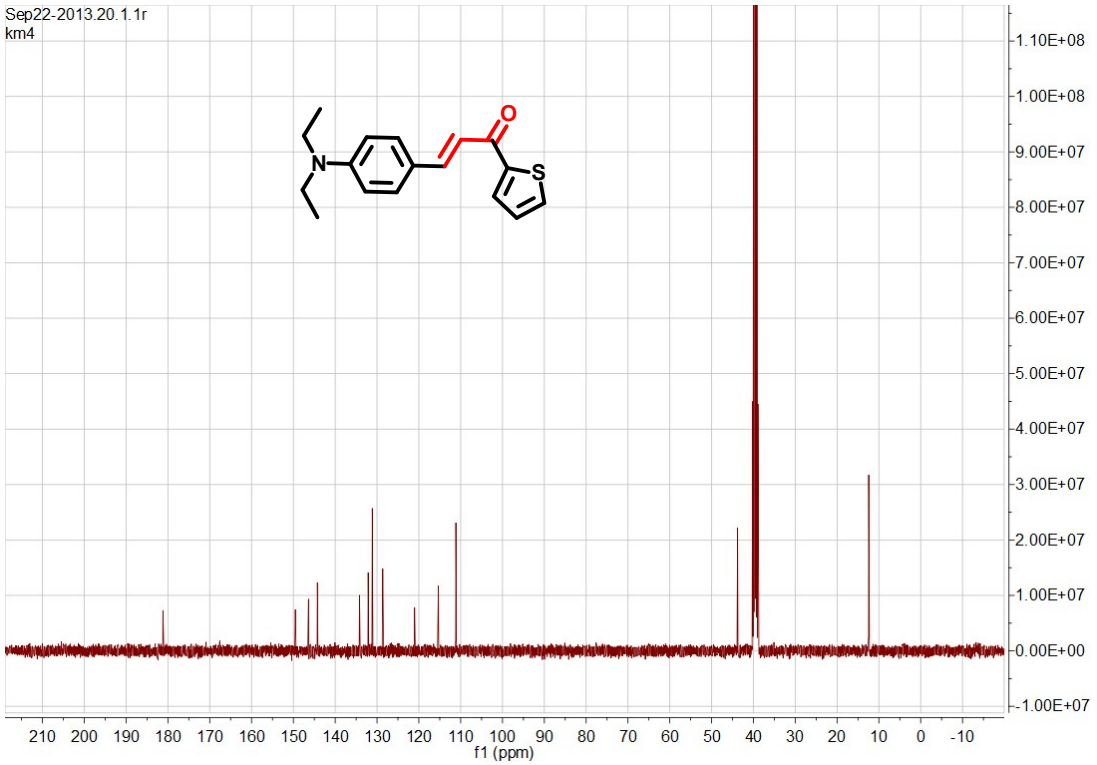

Figure S9. ^{13}C NMR of **XT1**

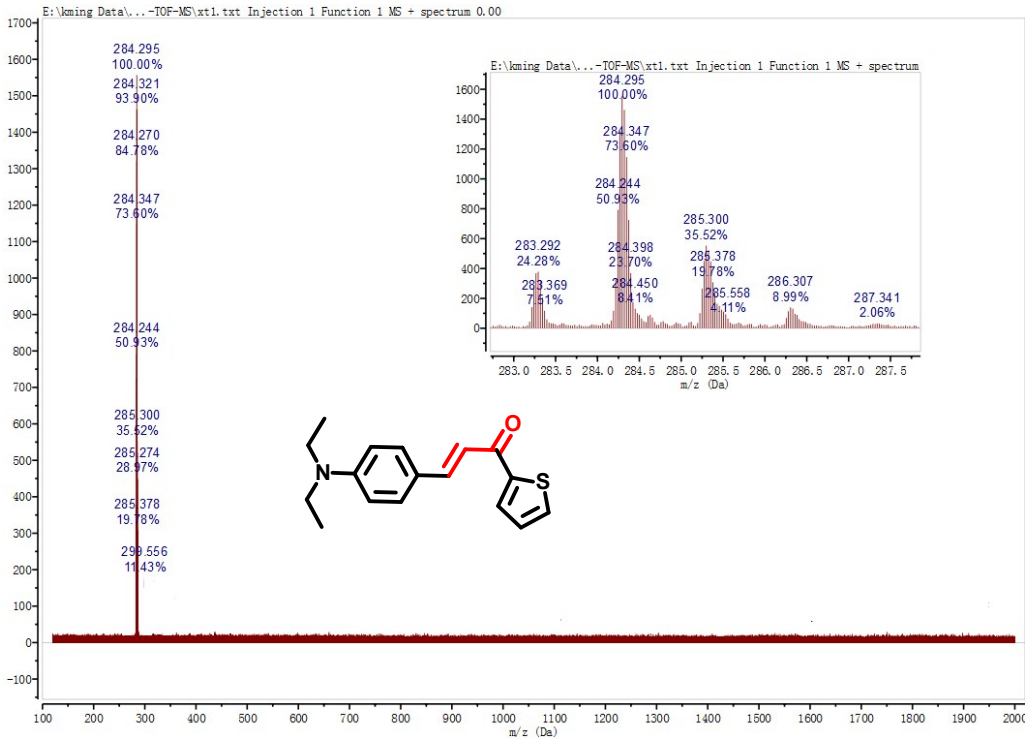

Figure S10. MALDI-TOF-MS of **XT1**

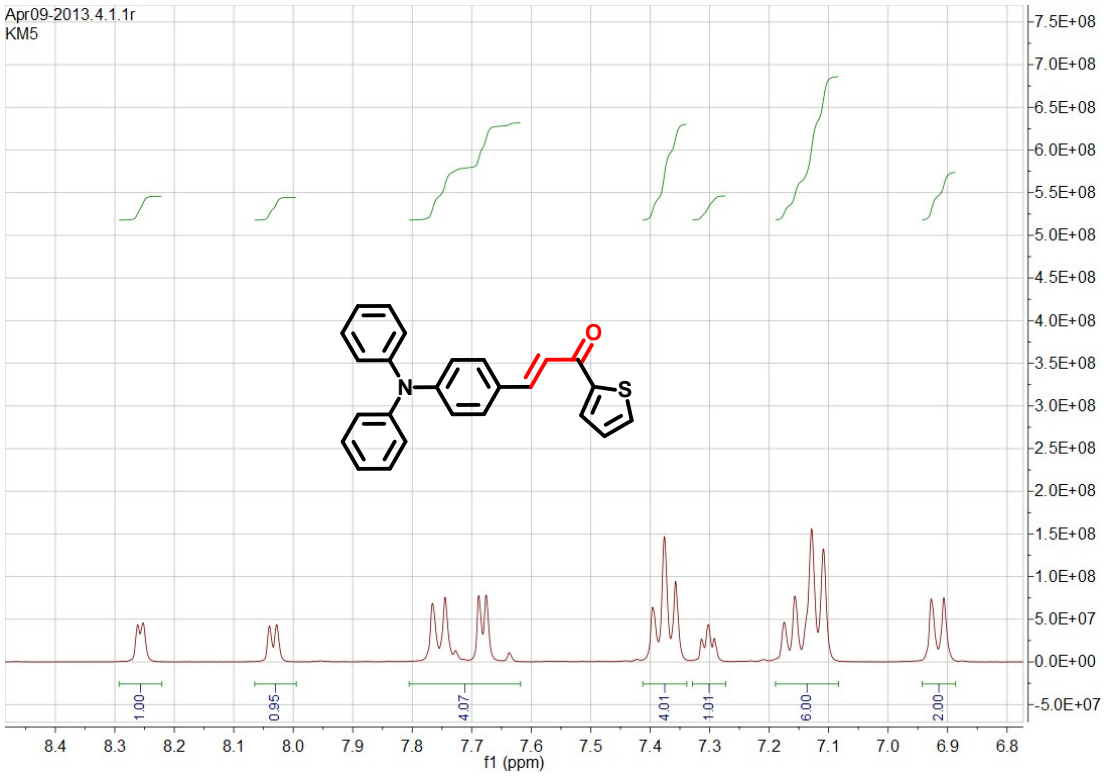

Figure S11. ^{1}H NMR of **XT2**

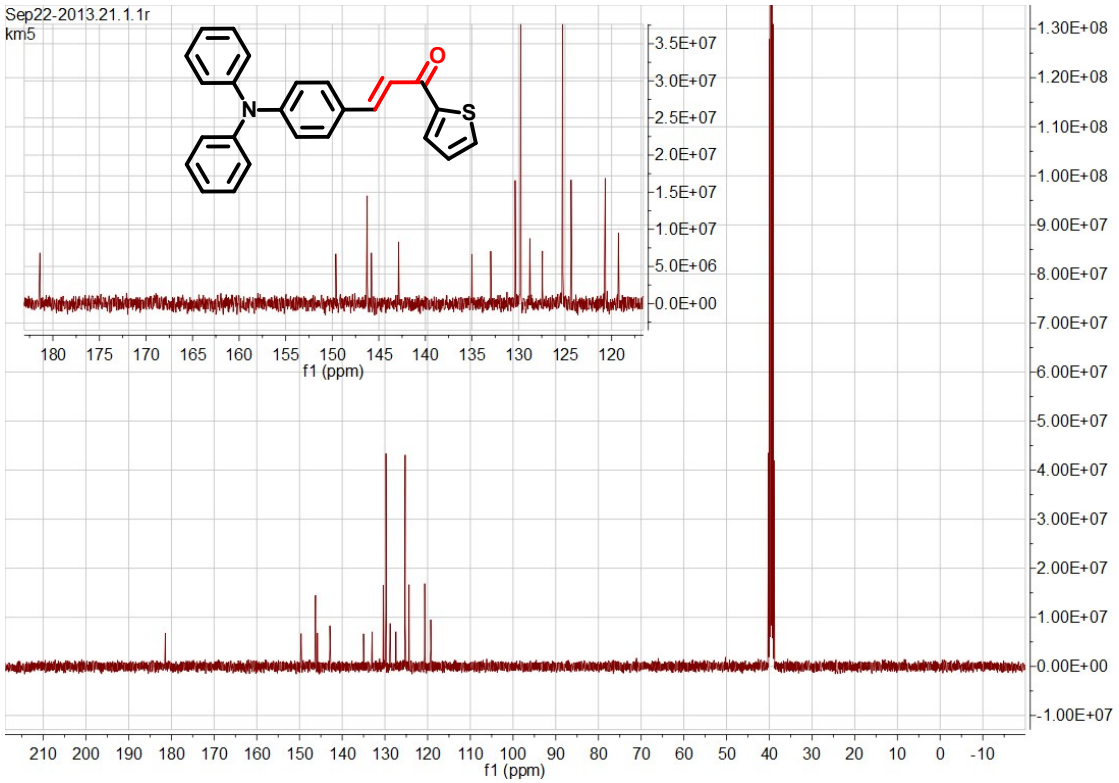

Figure S12. ^{13}C NMR of **XT2**

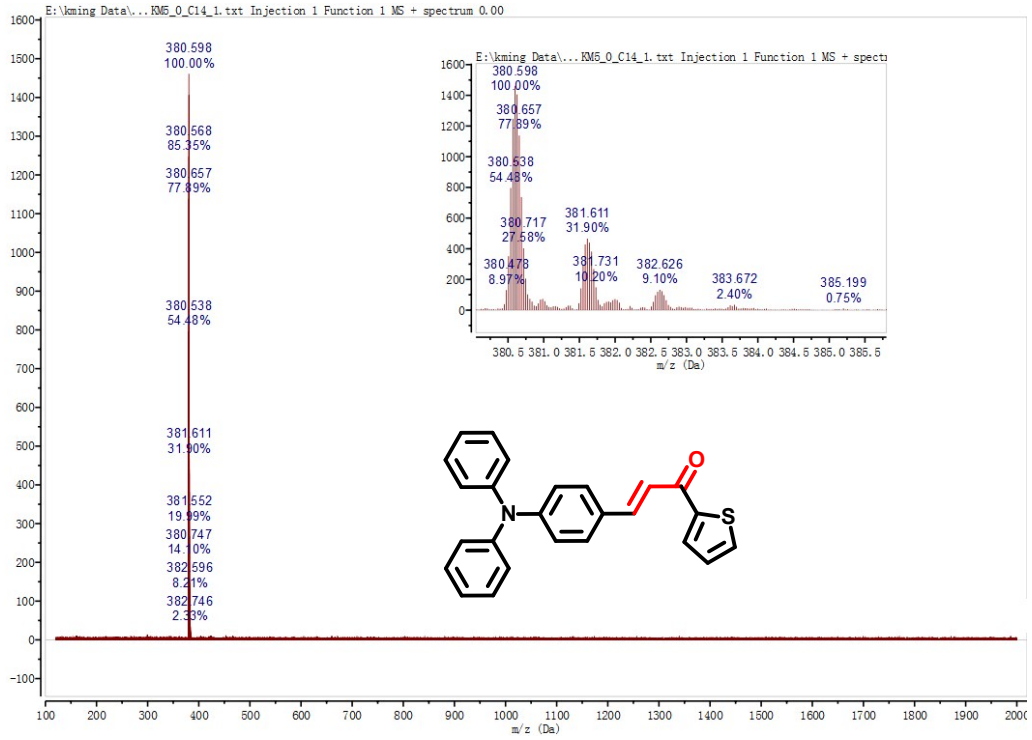

Figure S13. MALDI-TOF-MS of **XT2**

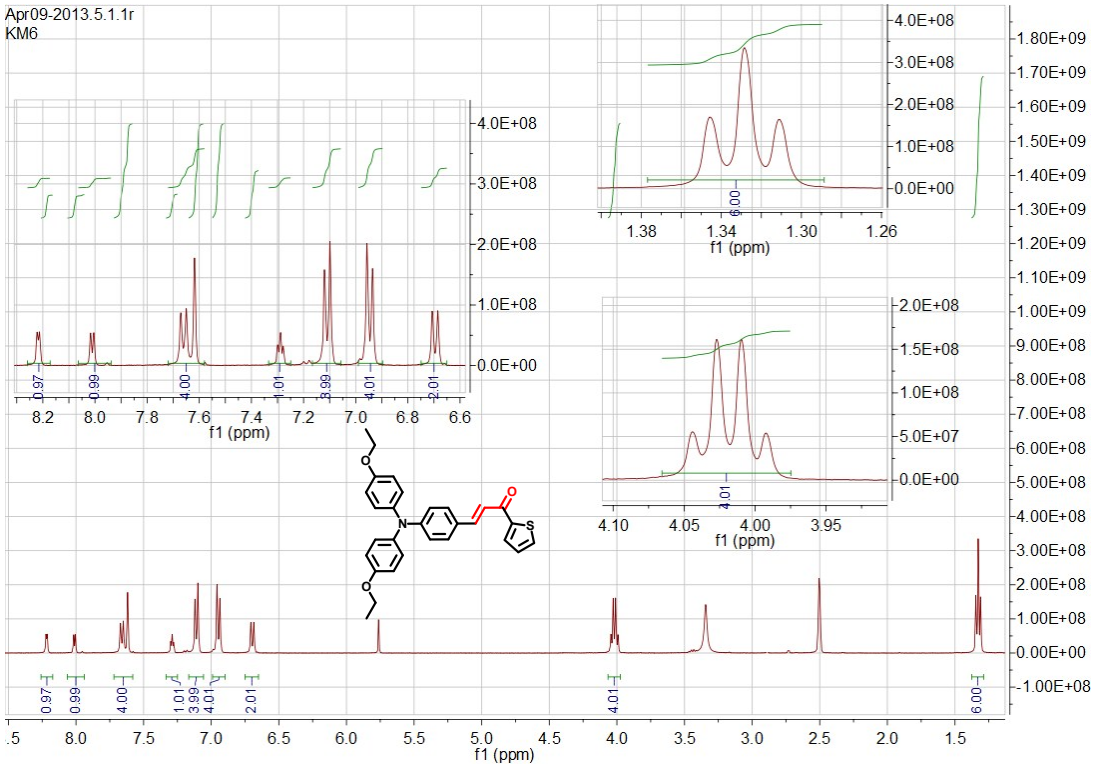

Figure S14. ^{1}H NMR of **XT3**

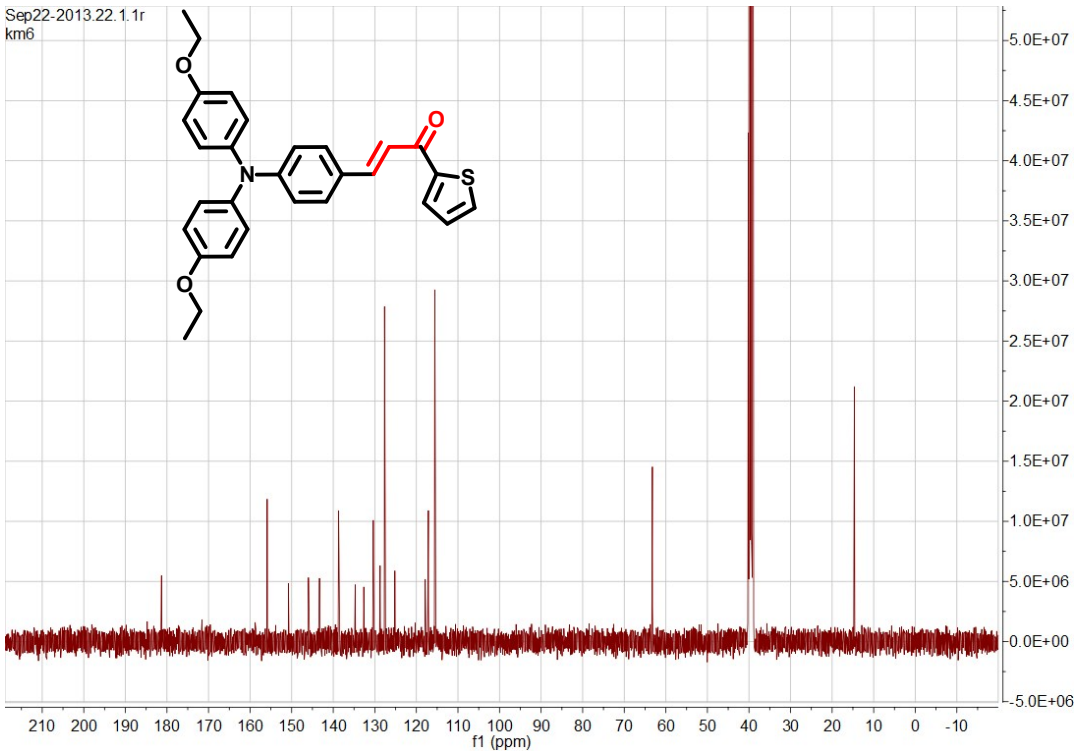

Figure S15. ^{13}C NMR of **XT3**

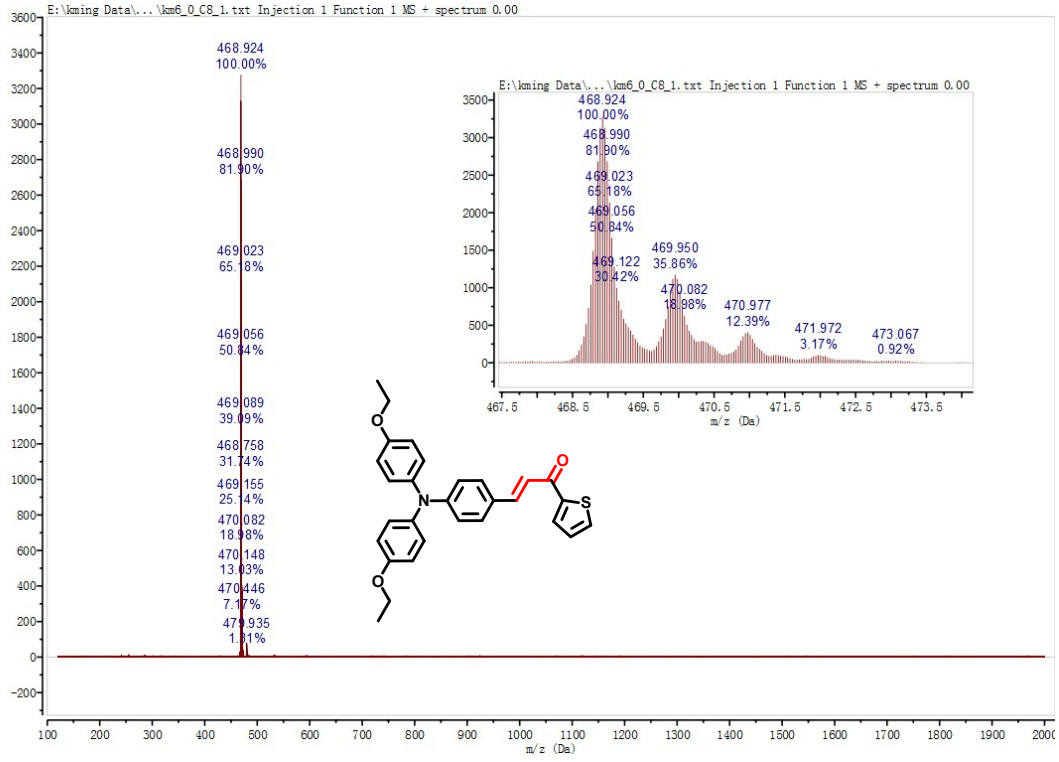

Figure S16. MALDI-TOF-MS of **XT3**

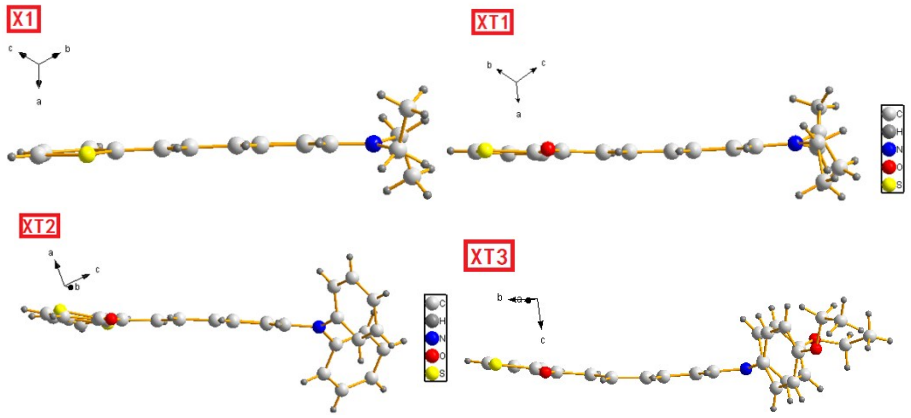

Figure S17. Alternative views of **X1**, **XT1**, **XT2** and **XT3** showing the quasi-planarity of terminal moieties.

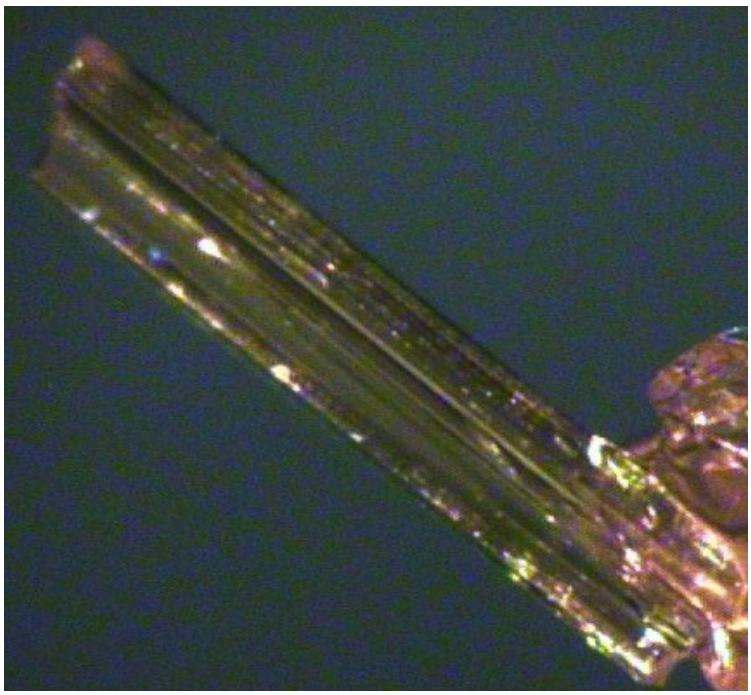

Figure S18. The crystal photograph of **XT1**

Table S1 Selected bond lengths (Å) and angles (°) for **X1**

C(1)-H(1A)	0.9600	C(5)-N(1)-C(2)	121.6(2)
C(2)-H(2A)	0.9700	C(5)-N(1)-C(4)	122.6(2)
C(2)-C(1)	1.511(4)	C(2)-N(1)-C(4)	115.8(2)
C(4)-C(3)	1.513(5)	C(6)-C(7)-C(10)	122.9(2)
C(4)-H(4A)	0.9700	C(6)-C(7)-H(7)	118.6
C(6)-H(6)	0.9300	C(7)-C(10)-C(9)	115.9(3)
C(10)-C(9)	1.398(4)	C(7)-C(10)-C(11)	118.8(2)
C(10)-C(11)	1.472(4)	C(9)-C(10)-C(11)	125.3(3)
C(11)-C(12)	1.333(4)	C(12)-C(11)-C(10)	126.6(3)
C(12)-C(13)	1.462(4)	C(12)-C(11)-H(11)	116.7
C(12)-H(12)	0.9300	C(10)-C(11)-H(11)	116.7

C(11)-H(11)	0.9300	N(1)-C(4)-C(3)	113.9(3)
C(9)-H(9)	0.9300	N(1)-C(4)-H(4A)	108.8
C(8)-H(8)	0.9300	C(11)-C(12)-C(13)	126.0(3)
C(12)-C(13)-S(1)	124.7(2)	C(11)-C(12)-H(12)	117.0
C(14)-C(13)-C(12)	123.9(3)	C(13)-C(12)-H(12)	117.0

Table S2 Selected π···π, C-H···π Interactions and potential hydrogen bonds in **X1**

π···π interactions			
R(i)-R(j)	Dihedral angel(i,j)(°)	⊥distance between the centroid(Å)	
R(1)-R(1)$^{(I)}$	47	5.977	
R(1)-R(2)$^{(II)}$	3.07	5.914	
R(1)-R(2)$^{(III)}$	74.61	5.035	
R(2)-R(1)$^{(IV)}$	3.07	5.913	
R(2)-R(1)$^{(III)}$	74.61	4.718	
R(2)-R(2)$^{(V)}$	72	5.023	
hydrogen bond			
	d(H ···S)	d(C ···S)	∠CHS(°)
C(11) -H(11) ···S(1)	2.85	3.248	107
C-H···π Interactions			
	H···R(2)(Å)	∠C-H···R(2)(°)	C···R(2)(Å)
C(14)-H(14)→R(2)(VI)	2.69	153	3.563

Symmetry code:(I)1-X,1/2+Y,5/2-Z;(II)X,-1+Y,Z;(III)1/2+X,-1/2-Y,2-Z;(IV)X,1+Y,Z;(V) -1/2+X,1/2-Y,2-Z;(VI):-1/2+X,-1/2-Y,2-Z;R(1):S(1)-C(13)-C(14)-C(15)-C(16);R(2) :C(5)-C(6)-C(7)-C(10)-C(9)-C(8)

Table S3 Selected bond lengths (Å) and angles (°) for **XT1**

C(4)-C(5)	1.469(5)	C(5)-C(4)-S(1)	118.9(2)
C(5)-O(1)	1.232(4)	O(1)-C(5)-C(6)	122.3(3)
C(5)-C(6)	1.449(5)	O(1)-C(5)-C(4)	119.5(3)
C(6)-C(7)	1.330(5)	C(6)-C(5)-C(4)	118.2(3)
C(7)-C(8)	1.450(5)	C(7)-C(6)-C(5)	121.2(3)
C(6)-H(6)	0.9300	C(7)-C(6)-H(6)	119.4
C(7)-H(7)	0.9300	C(5)-C(6)-H(6)	119.4
C(8)-C(9)	1.385(4)	C(6)-C(7)-C(8)	129.2(3)
C(9)-C(10)	1.370(5)	C(6)-C(7)-H(7)	115.4
C(9)-H(9)	0.9300	C(8)-C(7)-H(7)	115.4
C(10)-C(11)	1.406(5)	C(9)-C(8)-C(7)	124.3(3)
C(11)-N(1)	1.370(5)	C(13)-C(8)-C(7)	119.2(3)
C(16)-N(1)	1.453(4)	C(10)-C(9)-C(8)	122.2(3)
C(16)-C(17)	1.490(6)	C(8)-C(9)-H(9)	118.9

Table S4 Selected π···π, C-H···π Interactions and potential hydrogen bonds in **XT1**

π···π interactions		
R(i)-R(j)	Dihedral angel(i,j)(°)	⊥distance between the centroid(Å)
R(1)-R(1)$^{(I)}$	67	5.079
R(1)-R(2)$^{(II)}$	89.98	5.236
R(2)-R(1)$^{(III)}$	58.31	4.782
R(2)-R(1)$^{(IV)}$	89.98	5.236
hydrogen bonds		
	d(H···O)	d(C···O)	∠CHS(°)
C(7)-H(7)···O(1)	2.45	2.799	102
C(16)-H(16B)···O(1)	2.55	3.497	166
C-H···π Interactions			
	H···R(2)(Å)	∠C-H···R(2)(°)	C···R(2)(Å)
C(15')-H(15E)→R(2)(V)	2.89	128	3.559

Symmetry code:(I)-1/2+X,Y,1/2-Z;(II)1/2-X,1/2+Y,Z;(III)1-X,-1/2+Y,1/2-Z;(IV) 1/2-X,-1/2+Y,Z;(V)1/2+X,1/2-Y,1-Z;S(1)-C(1)-C(2)-C(3)-C(4);R(2) :C(8)-C(9)-C(10)-C(11)-C(12)-C(13)

Table S5 Selected bond lengths (Å) and angles (°) for **XT2**

C(1)-C(6)	1.378(2)	C(20)-H(20)	0.9300
C(1)-C(2)	1.381(3)	C(20)-C(21)	1.469(2)
C(1)-N(1)	1.423(2)	C(21)-O(1)	1.2273(19)
C(7)-N(1)	1.429(2)	C(21)-C(22)	1.505(18)
C(2)-C(3)	1.384(3)	C(23)-C(22)-S(1)	113.6(13)
C(13)-C(14)	1.394(2)	C(23)-C(22)-C(21)	121.3(12)
C(14)-C(15)	1.376(2)	C(21)-C(22)-S(1)	125.0(10)
C(15)-C(16)	1.393(2)	O(1)-C(21)-C(22)	119.2(6)
C(14)-H(14)	0.9300	O(1)-C(21)-C(20)	121.87(15)
C(15)-H(15)	0.9300	C(21)-C(20)-H(20)	119.7
C(16)-C(19)	1.457(2)	C(19)-C(20)-C(21)	120.55(15)
C(19)-H(19)	0.9300	C(20)-C(19)-H(19)	115.3
C(19)-C(20)	1.329(2)	C(20)-C(19)-C(16)	129.35(15)
C(17)-C(16)-C(19)	123.96(14)	C(15)-C(16)-C(19)	118.71(14)
		C(16)-C(19)-H(19)	115.3

Table S6 Selected π···π, C-H···π Interactions and potential hydrogen bonds in **XT2**

π···π interactions		
R(i)-R(j)	Dihedral angel(i,j)(˚)	⊥distance between the centroid(Å)
R(1)-R(1)$^{(I)}$	0	4.976
R(1)-R(2)$^{(I)}$	5.5	4.874
R(1)-R(3)$^{(II)}$	63.4	4.973
R(1)-R(5)$^{(III)}$	5.0	5.451
R(1)-R(5)$^{(II)}$	5.0	4.851
R(1)-R(5)$^{(I)}$	5.0	5.492
R(2)-R(2)$^{(I)}$	0	4.77
R(2)-R(5)$^{(II)}$	9.4	4.815
R(4)-R(4)$^{(IV)}$	0	5.333
R(5)-R(4)$^{(V)}$	61.76	5.134

hydrogen bonds			
D-H···A	d(H···A)	d(D···A)	∠DHA(˚)
C(12)-H(12)···O(1)	2.56	3.489	173
C(19)-H(19)···O(1)	2.43	2.795	103
C(20)-H(20)···S(1)	2.79	3.175	106
C(25)-H(25)···O(1)	2.39	3.289	162

C-H···π Interactions			
	H···R(4)(Å)	∠C-H···R(4)(˚)	C···R(2)(Å)
C(5)-H(5)→R(4)(VI)	2.79	149	3.613

Symmetry code:(I)2-X,-1-Y,1-Z;(II)1-X,-Y,1-Z;(III)1-X,-1-Y,1-Z;(IV)-X,-Y,2-Z;(V) 1+X,Y,Z;(VI) X,1+Y,Z;R(1) S(1)-C(22)-C(23)-C(24)-C(25);R(2) : S(1') C(22') C(23') C(24') C(25');R(3): C(1)-C(2)-C(3)-C(4)-C(5)-C(6);R(4):C(7)-C(8)-C(9)-C(10)-C(11)-C(12);R(5):C(13)-C(14)-C(15)-C(16)-C(17)-C(18);

Table S7 Selected bond lengths (Å) and angles (°) for **XT3**

S(1)-C(26)	1.707(4)	C(27)-C(26)-S(1)	110.1(3)
C(26)-C(27)	1.358(5)	C(25)-C(26)-S(1)	118.9(3)
C(26)-C(25)	1.454(5)	C(27)-C(26)-C(25)	131.0(4)
C(25)-O(3)	1.230(4)	O(3)-C(25)-C(26)	120.5(4)
C(25)-C(24)	1.474(5)	C(26)-C(25)-C(24)	117.4(4)
C(23)-C(24)	1.323(5)	O(3)-C(25)-C(24)	122.1(4)
C(23)-C(22)	1.448(5)	C(25)-C(24)-H(24)	118.9
C(24)-H(24)	0.9300	C(23)-C(24)-H(24)	118.9
C(23)-H(23)	0.9300	C(24)-C(23)-H(23)	115.9
N(1)-C(17)	1.382(5)	C(22)-C(23)-H(23)	115.9
N(1)-C(16)	1.440(5)	C(21)-C(22)-C(23)	122.1(4)
N(1)-C(8)	1.433(5)	C(19)-C(22)-C(23)	121.5(4)
C(24)-C(23)-C(22)	128.2(4)	C(23)-C(24)-C(25)	122.2(4)

Table S8 Selected π···π, C-H···π Interactions and potential hydrogen bonds in **XT3**

π···π interactions		
R(i)-R(j)	Dihedral angel(i,j)(°)	⊥distance between the centroid(Å)
R(1)-R(2)$^{(I)}$	57.4	5.358
R(1)-R(4)$^{(II)}$	14.1	4.208
R(1)-R(5)$^{(III)}$	15.7	5.656
R(5)-R(5)$^{(IV)}$	0	5.273
R(6)-R(6)$^{(V)}$	0	5.424

hydrogen bonds			
D-H···A	d(H···A)	d(D···A)	∠DHA(°)
C(23)-H(23)···O(3)	2.50	2.835	101
C(43)-H(43)···O(1)	2.58	3.410	149
C(52)-H(52)···O(6)	2.48	2.821	102

C-H···π Interactions			
	H···R(Å)	∠C-H···R(°)	C···R(Å)
C(1)-H(1C)→R(1)	2.90	163	3.828
C(15)-H(15)→R(8)	2.97	157	3.848
C(36)-H(36)→R(4)	2.95	151	3.791

Symmetry code:(I)3/2-X,-1/2+Y,3/2-Z;(II)1-X,-Y,1-Z;(III)-1/2+X,1/2-Y,1/2+Z;(IV) 1-X,1-Y,2-Z;(V)1-X,-Y,2-Z;R(1):S(1)-C(26)-C(27)-C(28)-C(29);R(2):C(3)-C(4)-C(5)-C(8)-C(7)-C(6);R(3):C(11)-C(12)-C(13)-C(16)-C(15)-C(14);R(4):C(17)-C(18)-C(19)-C(22)-C(21)-C(20);R(5): S(2)-C(55)-C(56)-C(57)-C(58);R(6) C(32)-C(33)-C(34)-C(37)-C(36)-C(35);R(8) C(46)-C(47)-C(48)-C(51)-C(50)-C(49).

Table S9 Single-photon-related photophysical properties of six dyes in different solvents.

Compounds	Solvents	$\lambda_{max}{}^{a}(\varepsilon_{max}{}^{b})$		$\lambda_{max}{}^{c}$	$\Delta\nu^{d}$	Φ^{e}	τ/ns
	Benzene	360(1.84)		419	59	0.023	0.59
	Dichloromethane	361(1.74)		443	82	0.017	0.37
	Tetrahydrofuran	362(1.77)		433	71	0.030	~
X1	Ethyl acetate	357(1.72)		432	75	0.023	0.42
	Ethanol	353(1.61)		442	89	0.040	0.37
	Acetonitrile	357(1.67)		451	94	0.017	0.38
	DMF	363(1.09)		453	90	0.029	~
	Benzene	302(2.43)	373(2.25)	425	52	0.240	1.42
	Dichloromethane	303(2.26)	374(2.82)	453	79	0.265	2.33
	Tetrahydrofuran	302(2.40)	372(2.78)	440	68	0.260	~
X2	Ethyl acetate	301(1.94)	368(2.05)	438	70	0.225	1.78
	Ethanol	301(1.79)	368(1.97)	445	77	0.326	2.12
	Acetonitrile	301(2.17)	369(2.88)	462	93	0.218	2.80
	DMF	303(1.68)	373(2.57)	461	88	0.263	~
	Benzene	303(1.70)	388(2.59)	463	75	0.147	2.89
	Dichloromethane	302(1.81)	387(2.99)	511	124	0.077	4.65

	Tetrahydrofuran	301(1.71)	386(2.76)	491	105	0.116	~
X3	Ethyl acetate	300(1.95)	382(3.16)	490	108	0.095	3.83
	Ethanol	301(1.62)	382(2.72)	506	124	0.039	2.75
	Acetonitrile	300(1.69)	381(3.11)	521	140	0.018	2.31
	DMF	301(1.57)	385(3.10)	520	135	0.034	~
	Benzene	282(2.22)	428(3.20)	480	52	0.016	0.65
	Dichloromethane	287(1.76)	435(3.75)	525	90	0.055	2.62
	Tetrahydrofuran	285(1.17)	425(2.57)	508	83	0.069	~
XT1	Ethyl acetate	283(1.66)	421(3.79)	518	97	0.036	1.96
	Ethanol	280(1.59)	437(4.06)	550	113	0.002	0.15
	Acetonitrile	280(1.24)	429(3.46)	539	110	0.018	0.74
	DMF	286(1.26)	433(3.92)	534	101	0.038	~
	Benzene	300(2.95)	422(2.95)	497	75	0.091	2.62
	Dichloromethane	300(3.74)	426(4.53)	557	131	0.022	3.74
	Tetrahydrofuran	299(2.76)	416(3.21)	523	107	0.073	~
XT2	Ethyl acetate	298(2.70)	413(3.36)	530	117	0.027	3.02
	Ethanol	298(2.59)	425(3.23)	533	108	0.0006	0.14
	Acetonitrile	297(2.73)	417(3.53)	575	158	0.002	0.62
	DMF	300(2.45)	421(3.28)	564	143	0.006	~
	Benzene	299(2.97)	435(3.21)	546	111	0.020	2.27
	Dichloromethane	299(2.98)	439(3.64)	—	—	—	~
	Tetrahydrofuran	295(2.85)	426(3.38)	574	148	0.003	~
XT3	Ethyl acetate	295(2.58)	426(3.19)	576	150	0.0003	0.51
	Ethanol	296(2.41)	441(3.08)	—	—	—	~
	Acetonitrile	295(2.81)	428(3.85)	—	—	—	~
	DMF	299(2.01)	433(2.97)	—	—	—	~

[a] Absorption peak position in nm. [b] Maximum molar extinction coefficient in 10^4 mol^{-1} L cm^{-1}. [c] Peak position of SPEF, exited at the maximum wavelength of absorption. [d] Stokes shift in nm. [e] Quantum yields determined by using quinine sulfate as standard. —Fluorescence quenching.

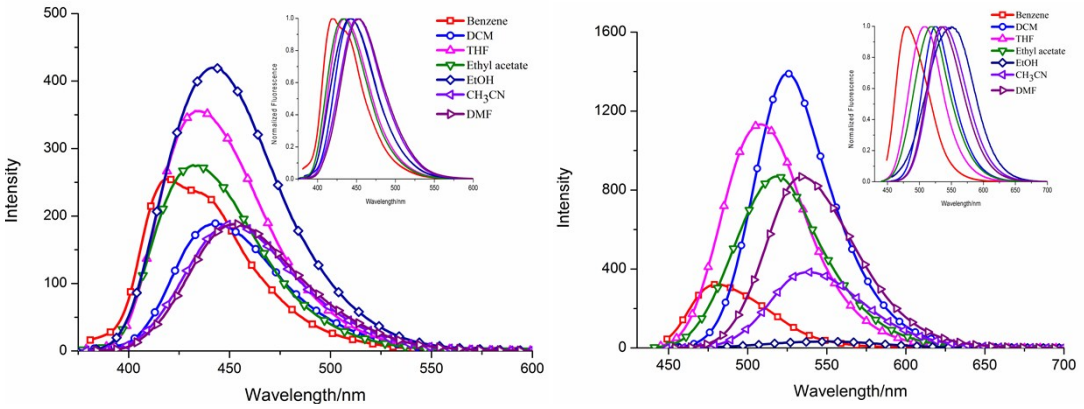

Figure S19. Fluorescence spectra of dyes **X1**(left) and **XT1**(right) in different solvents of different polarities with a concentration of 1.0×10^{-5} mol/L.

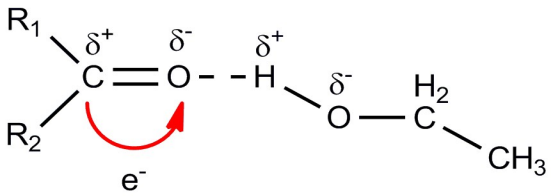

Figure S20. The formation process of hydrogen bond.

Table S10 Selected experimental and calculated optical data for the dyes

Compd.	OI[a]	ΔE(eV)[b]	Cal.λ_{max} (nm)[c]	Obs.λ_{max} (nm)[d]	f[e]	Character
X1	HOMO→LUMO	3.4008	365	353	1.0508	ICT/π→π*
X2	HOMO→LUMO+2	4.0663	305	301	0.1533	π→π*
	HOMO→LUMO	3.2578	381	368	1.1358	ICT/π→π*
X3	HOMO→LUMO+3	4.2192	294	301	0.0988	π→π*
	HOMO→LUMO	3.3595	369	382	1.2417	ICT/π→π*
XT1	HOMO→LUMO+1	4.4290	280	280	0.0644	n→π*/π→π*
	HOMO→LUMO	2.8728	432	437	0.8660	ICT/π→π*
XT2	HOMO→LUMO+3	4.2534	291	298	0.1694	π→π*
	HOMO→LUMO	2.7400	452	425	0.8023	ICT/π→π*
XT3	HOMO→LUMO+3	4.2671	291	296	0.0878	π→π*
	HOMO→LUMO	2.7798	446	441	0.8393	ICT/π→π*

[a]Orbitals involved in the excitations, [b]Excitation energies (eV), [c]Calculated peak position of the longest absorption band in ethanol, [d] Observed peak position of the longest absorption band in ethanol , [f]Oscillator Strengths

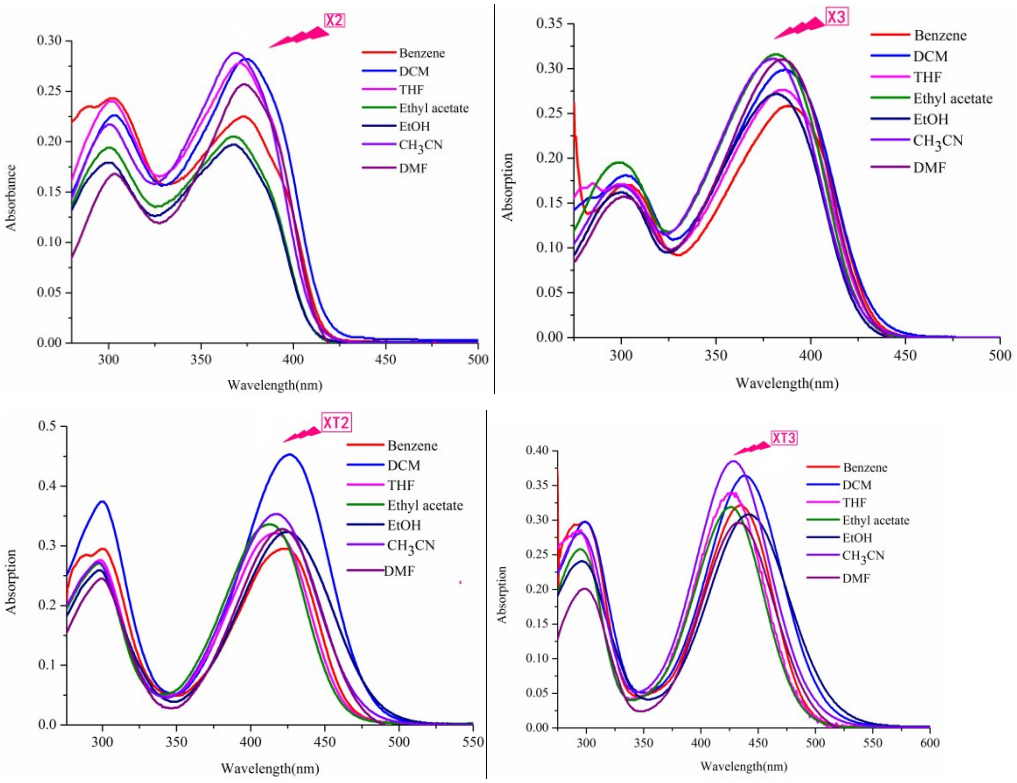

Figure S21. Absorption spectra of dyes **X2, X3, XT2** and **XT3** in different solvents of different polarities with a concentration of 1.0×10^{-5} mol/L.

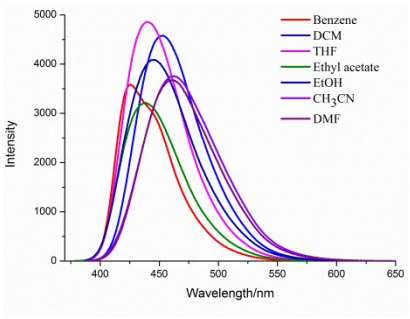

Figure S22. Fluorescence spectra of dye **X2** in different solvents of different polarities with a concentration of 1.0×10^{-5} mol/L

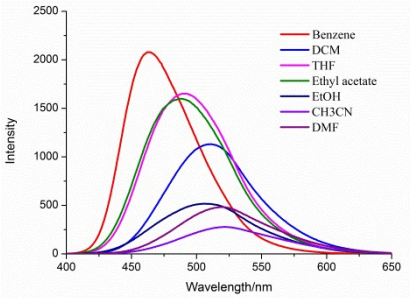

Figure S23. Fluorescence spectra of dye **X3** in different solvents of different polarities with a concentration of 1.0×10^{-5} mol/L

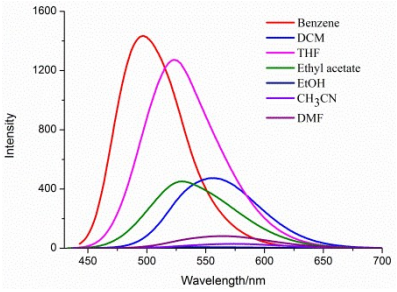

Figure S24. Fluorescence spectra of dye **XT2** in different solvents of different polarities with a concentration of 1.0×10^{-5} mol/L

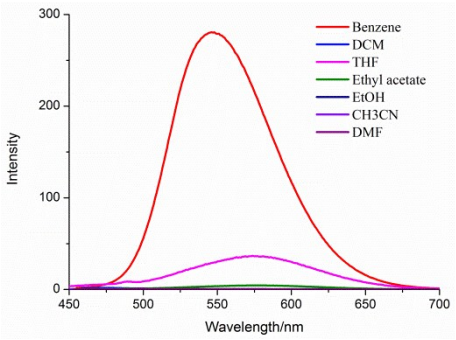

Figure S25. Fluorescence spectra of dye **XT3** in different solvents of different polarities with a concentration of 1.0×10^{-5} mol/L

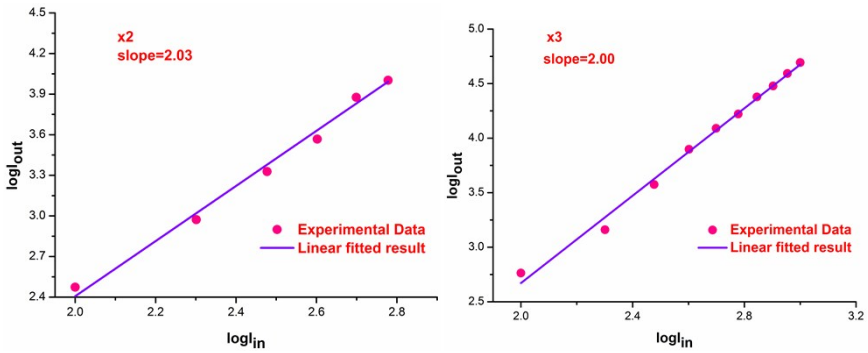

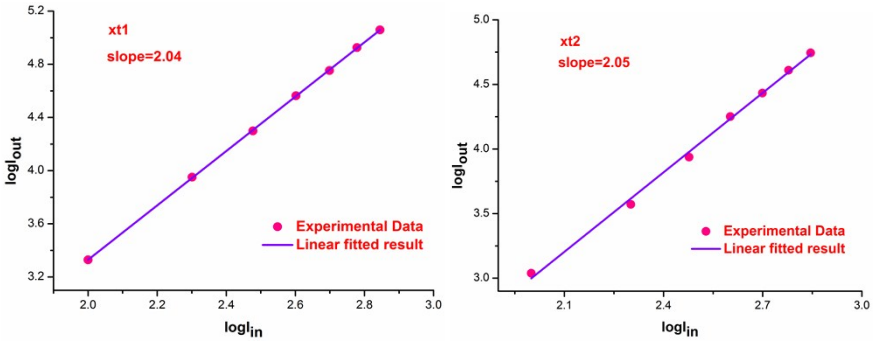

Figure S26. Two-photon absorption verification of **X2**, **X3**, **XT1** and **XT2** which I_{in} and I_{out} represent the input laser power and output fluorescence, respectively.

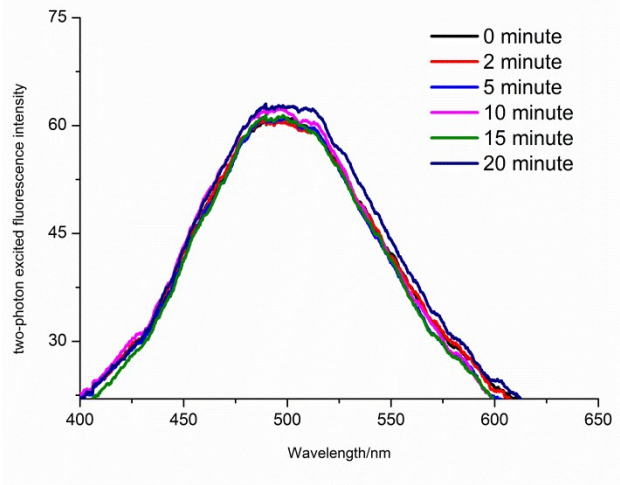

Figure S27. Time-dependent two-photon excited fluorescence of **X2** excited at 790 nm in DMF.

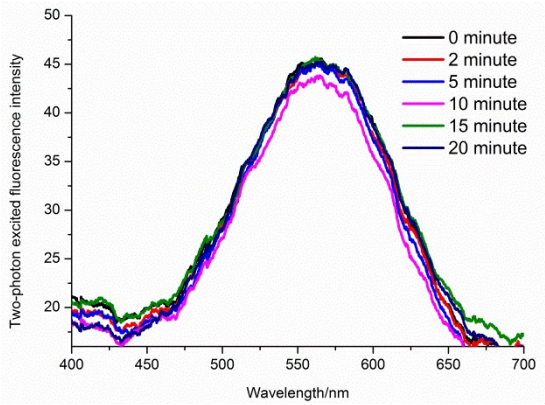

Figure S28. Time-dependent two-photon excited fluorescence of **X3** excited at 790 nm in DMF.

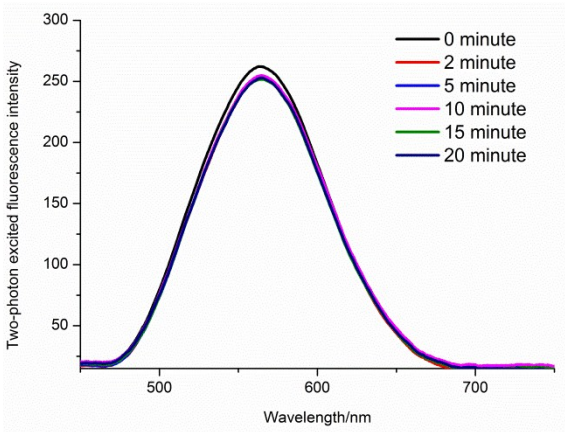

Figure S29. Time-dependent two-photon excited fluorescence of **XT1** excited at 830 nm in DMF.

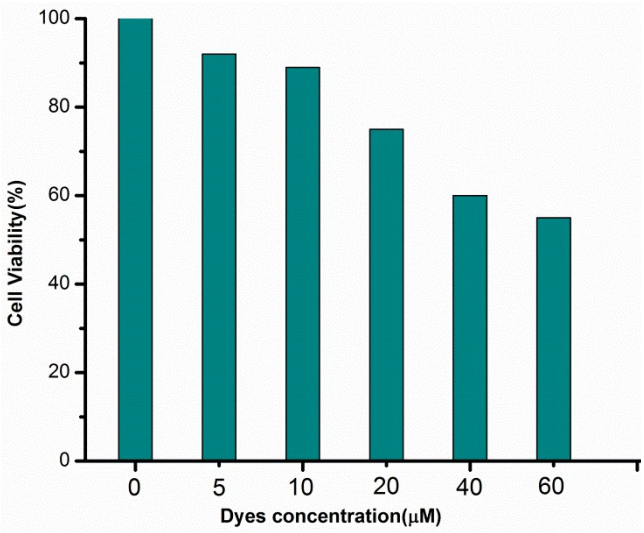

Figure S30. MTT assay of HepG2 cells incubate with dyes **X2** at different concentrations for 24h.

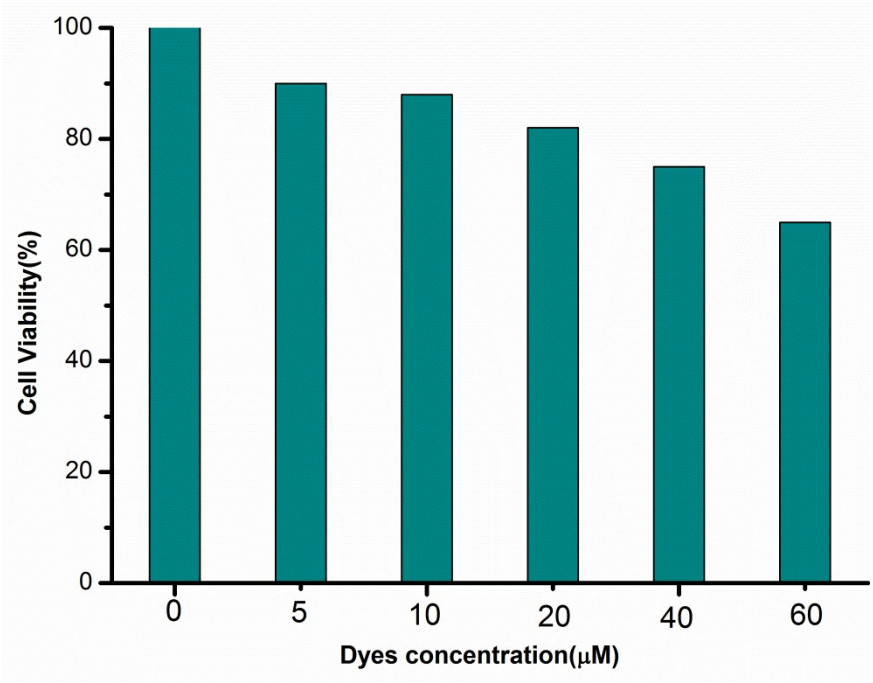

Figure S31. MTT assay of HepG2 cells incubate with dyes **XT1** at different concentrations for 24h.